Virus Research 267 (2019) 26–35

Contents lists available at ScienceDirect

Virus Research

journal homepage: www.elsevier.com/locate/virusres

Functional insights into the role of C-terminal disordered domain of Sesbania mosaic virus RNA-dependent RNA polymerase and the coat protein in viral replication *in vivo*

Arindam Bakshi, Handanahal Subbarao Savithri*

Department of Biochemistry, Indian Institute of Science, Bangalore, 560012, India

ARTICLE INFO

Keywords:
Sesbania mosaic virus
RNA-dependent RNA polymerase
P10
Coat protein
Motif E

ABSTRACT

The C-terminal disordered domain of sesbania mosaic virus (SeMV) RNA-dependent RNA polymerase (RdRp) interacts with the viral protein P10. The functional significance of this interaction in viral replication was examined by a comparative analysis of genomic and sub-genomic RNA levels (obtained by quantitative real time PCR) in the total RNA extracted from *Cyamopsis* plants agro-infiltrated with wild-type or mutant forms of SeMV infectious cDNA (icDNA). The sgRNA copy numbers were found to be significantly higher than those of gRNA in the wild-type icDNA transfected plants. Transfection of a mutant icDNA expressing an RdRp lacking the C-terminal disordered domain led to a drastic reduction in the copy numbers of both forms of viral RNA. This could be due to the loss of interaction between the disordered domain of RdRp and P10 and possibly other viral/host proteins that might be required for the assembly of viral replicase. The C-terminal disordered domain also harbours the motif E which is essential for the catalytic function of RdRp. Mutation of the conserved tyrosine within this motif in the full length icDNA resulted in complete inhibition of progeny RNA synthesis in the transfected plants confirming the importance of motif E in the polymerase function *in vivo*. The role of coat protein (CP) in viral infection was also investigated by agro-infiltration of a CP start codon mutant icDNA which suggested that CP is essential for the encapsidation of viral progeny RNAs at later stages of infection.

1. Introduction

Positive-sense RNA viruses represent the largest group of plant viruses and are known to replicate their genome within host derived membrane-bound vesicles termed as viral replication complexes (VRCs). These VRCs facilitate the sequestration of the viral RNA and viral proteins along with several host proteins and lipids which create a favourable environment for replication (Shulla and Randall, 2016). The assembly of these complexes are reported to be orchestrated by the interactions between viral RNA-dependent RNA polymerase (RdRp) and various other viral-encoded ancillary proteins as well as co-opted host factors (de Castro et al., 2013; den Boon et al., 2010; Nagy and Pogany, 2011).

Sesbania mosaic virus (SeMV), a member of the genus *Sobemovirus* is a sap-transmissible positive-sense RNA virus which infects *Sesbania grandiflora* pers agathi, in the farmer's field around Tirupati, Andhra Pradesh in India. The SeMV genome is 4148 nts long which consists of three overlapping open reading frames (ORFs) and has a covalently linked viral protein (VPg) at its 5' end (Lokesh et al., 2001) (Fig S1). The 5' and the 3' proximal ORFs code for the movement protein (MP) and coat protein (CP) respectively. The central ORF (ORF-2) codes for two polyproteins, 2a and 2ab. The ORF-2a codes for polyprotein 2a with the domain arrangement: membrane anchor (TM)-protease-VPg-P10-P8 domain. The ORF-2b codes for the RNA-dependent RNA polymerase (RdRp) which is expressed as polyprotein 2ab with the domain arrangement: TM-protease-VPg-RdRp (Nair and Savithri, 2010; Satheshkumar et al., 2004) (Fig. S1). This domain arrangement is conserved across sobemoviruses. However, not much is known about the functional role of viral-encoded ancillary proteins that could act as interacting partners for sobemoviral RdRps in virus multiplication *in vivo*.

We have previously reported that SeMV RdRp interacts strongly with the ORF-2a encoded P10 domain *via* the C-terminal disordered region of RdRp (Govind et al., 2014). The interaction was shown to positively modulate the polymerase activity of RdRp by preventing the aggregation of the protein *in vitro* (Bakshi et al., 2019). It is likely that the interaction between RdRp and P10 is crucial for the assembly of VRC and recruitment of other replication associated viral proteins or

* Corresponding author at: Department of Biochemistry, New Biological Sciences Building, Indian Institute of Science, Bengaluru, 560012, Karnataka, India.
E-mail address: hss@alumni.iisc.ac.in (H.S. Savithri).

https://doi.org/10.1016/j.virusres.2019.05.003
Received 15 February 2019; Received in revised form 24 April 2019; Accepted 2 May 2019
Available online 02 May 2019
0168-1702/

host factors *in vivo*. Further, a conserved sequence motif (motif E), present between 72–85 residues from the C-terminus of SeMV RdRp was found to be indispensable for the polymerase activity *in vitro* (Bakshi et al., 2019). Therefore, the functional significance of the RdRp-P10 interaction as well as the role of motif E in the synthesis of viral progeny RNAs was investigated in the present study. Furthermore, the 3'-proximal CP ORF in SeMV genome is translated *via* the subgenomic messenger RNA (sgRNA). Some viruses such as alfalfa mosaic virus (AMV) and related ilarviruses require CP, which is also translated *via* a subgenomic RNA, to initiate successful infection. It was demonstrated that the 3' UTR of AMV RNA 3 consists of a minimum of two independent CP-binding sites (Reusken et al., 1994). However, there are no reports pertaining to the functional role (if any) of SeMV CP in viral replication.

An infectious cDNA (icDNA) clone is essential for studying viral gene functions *in vivo*. The SeMV icDNA clone (termed as IC IV) was shown to be infectious in *Sesbania* (natural host) as well as *Cyamopsis* (experimental host) plants which could mimic the wild-type virus infection *in vivo* (Govind et al., 2012). In the present study, a mutant icDNA clone was generated by introducing a stop codon in the ORF-2b such that the C-terminal disordered domain of RdRp is deleted which could lead to the loss of interaction with P10. Similarly, the conserved tyrosine residue within the motif E of RdRp was mutated to alanine in the full length icDNA for studying the significance of this motif in polymerase activity of RdRp *in vivo*. These mutant icDNA clones were agro-infiltrated into *Cyamopsis* plants and the subgenomic (sgRNA) and genomic RNA (gRNA) synthesized at various time points post transfection were quantitated by real-time PCR (qPCR). A comparative analysis of these viral RNA levels with those of the wild-type icDNA transfected *Cyamopsis* plants demonstrated the importance of RdRp-P10 interaction *via* the C-terminal disordered region of RdRp in virus multiplication. Also, the motif E was shown to be crucial for the catalytic function of RdRp *in vivo*. Further, an analysis of the sgRNA and gRNA levels in CP start codon mutant icDNA transfected plants revealed that SeMV CP is not essential for viral replication but is required for the packaging of viral progeny RNAs.

2. Materials and methods

2.1. Agro-infiltration of SeMV icDNA constructs into Cyamopsis plants

Agro-infiltration was carried out essentially as described earlier (Eskelin et al., 2010). *Agrobacterium tumefaciens* strain C58C1 (Van Larebeke et al., 1974) containing the helper plasmid pGV2260 was transformed with the binary vector constructs. Transformation was carried out by electroporation (voltage 1.44 kV, conductivity 25 μF, and resistance 100- 200Ω). After electroporation, cells were grown in plain LB medium for 3–4 h at 28°C with vigorous shaking. The cells were harvested by centrifugation at 3000 g for 5 min and plated on LB agar plates containing kanamycin, carbenicilin and rifampicin (100 μg/ml each) and incubated at 30°C for 48 h. A single colony was inoculated to LB medium containing 10 mM MES pH 6.3 and 20 μM of acetosyringone and the antibiotics and grown at 30°C with shaking (200 rpm) until OD_{600} reached 0.6 − 0.8. The cells at this stage were harvested by centrifugation at 3000 g for 5 min and the pellet was washed with milli-Q water, followed by resuspension in induction buffer (10 mM MES pH 6.3, 10 mM $MgCl_2$, and 150 μM acetosyringone). The suspension was diluted with induction buffer to the desired density (OD_{600} 0.05–1.2) and incubated at room temperature for 3–4 h. The cotyledon leaves of *Cyamopsis tetragonoloba* plants to be infiltrated were turned upside down and a small prick was made with a needle in the middle of the intended infiltration area and the bacterial suspension was injected at this position with 1 ml syringe without needle.

2.1.1. Co-infiltration

Co-infiltration experiments were carried out by mixing *Agrobacterium* transformed with SeMV icDNA site directed mutants and *Agrobacterium* transformed with pEAQ ORF2 at OD_{600} of 0.8. This mixture was infiltrated onto plants as described above.

2.2. Western blot analysis

Leaf samples (100 mg) were homogenised in 500 μl of 50 mM phosphate buffered saline (PBS) pH 7.4. The crude extract [20 μl containing 400 μg of protein estimated using absorbance at 280 nm, (1.0 OD = 1 mg/ml)] was used for SDS-PAGE followed by western blot analysis. The SDS-PAGE was carried out at 125 V, for 2 h. After SDS-PAGE, proteins were electro-blotted on to PVDF membranes by applying a current of 100–150 mA for 2–3 h. Membrane was blocked with 5% skimmed milk solution (in PBS) for 1 h followed by incubation with primary antibody for 1 h. The blot was washed with phosphate/Tris buffered saline pH 7.5, 0.1% tween 20 (PBST). Finally, the blot was incubated with secondary antibodies for one hour followed by washing with PBST for 1 h (three times 20 min each). The blot was developed using ECL reagent.

2.3. RNA isolation

Transfected leaf samples (1.5 gm) were homogenised in liquid nitrogen and mixed with TRI-Reagent at a ratio of 1:10 (15 ml). The mixed slurry was kept in an end to end rotor at 4°C for 1–2 h. The tissue debris was removed by centrifugation at 13,000 rpm for 10 min. Equal volume of chloroform was added to the supernatant and mixed vigorously followed by centrifugation at 13,000 rpm for 10 min. The aqueous phase was carefully separated from the organic phase and 70% (v/v) of isopropanol was added and centrifuged at 13,000 rpm for 10 min to precipitate the RNA. The RNA was finally washed with 70% ethanol and dissolved in 100 μl of nuclease-free water. Absorbance was recorded at 260 nm to determine the concentrations of RNA samples.

2.4. First strand cDNA synthesis

The first strand cDNA was synthesized using equated concentrations (5 μg, as per absorbance at 260 nm) of total RNA isolated from the transfected leaf samples. Total RNA (5 μg) was annealed to DNA oligo nucleotide (60 pmol) specific to the viral gene sequence by heating at 72°C for 5–10 min and cooling on ice for 2 min. This was followed by addition of 1X buffer RT, 1 mM dNTPs, 1U/μl RNase inhibitor (RNaseIn), 1 μl of reverse transcriptase (RT) (200 U/μl) to the total reaction mixture (20 μl). The reaction mixture was incubated at 37°C for 5 min and at 42°C for one hour. The PCR was carried out using 1 μl of RT-reaction mixture in 50 μl PCR cocktail containing viral CP sense and antisense primers (Table S1), dNTPs and phusion polymerase to confirm the presence of viral RNA in the total RNA samples. The cDNA synthesized is proportional to the amount of viral RNA present in the sample. The same cDNA samples were used for quantitation of the viral RNA copy numbers by qPCR as described in the next section.

2.5. Quantitation of cDNA using qPCR

The qPCR reaction (20 μl) was set up using 10 μl of 10X SYBR green mix containing Taq DNA polymerase and dNTPs, 5 μl of template cDNA and 500 nM of sense and antisense primers. The amplicon size for the PCR was chosen to be around 100–150 bp since it increases the sensitivity of annealing and amplification in qPCR.

The SeMV icDNA cassette that includes CaMV double 35S promoter, Nos terminator and ribozyme was previously cloned in between two BamHI sites within the multiple cloning site (MCS) of pBSK + vector (Govind et al., 2012) and was named IC IV SK + . Initially, a qPCR was set up with IC IV SK + DNA at varying copy numbers (300 to 3 billion) as template using MP qPCR sense and antisense primers (Table S1) or CP qPCR sense and antisense primers (Table S1) respectively. The

standard curve was drawn for the MP amplicon and CP amplicon by plotting the average threshold cycle number (Ct) against the copy number of IC IV SK + DNA on a semi-logarithmic scale. Further, the melting temperature (T_m) was recorded for each amplicon. The T_m should be identical for the standards as well as the unknown samples for each set of primers. This would determine the reliability of the standard for measurements of copy numbers in test samples.

The copy numbers of the viral RNA obtained from wild-type/mutant icDNA transfected plants were calculated by plotting the average Ct values for respective samples on the standard curve. Since 5 µg of total RNA was used for RT reaction, the final copy number of viral RNAs were computed as viral RNA copies/µg of total RNA.

2.6. Site directed mutagenesis

The mutant constructs were generated by PCR based site directed mutagenesis (Weiner et al., 1994). PCR was performed with the full length SeMV icDNA clone (IC IV SK+) as template using appropriate sense and antisense primers and Phusion DNA polymerase. The list of primers used for the current study is tabulated (Table S1). The primer-template annealing was performed at various temperatures by gradient PCR to obtain optimum amplification. The PCR product was then digested with Dpn1 and transformed into competent *E.coli* DH5α cells. Plasmids were isolated from the positive transformants and initially screened by restriction digestion of the unique site incorporated in the mutagenic primers. The mutations were further confirmed by DNA sequencing. These mutant constructs in pBSK + were subsequently subcloned in pRD 400 binary vector within the BamH1 restriction site and used for the agro-infiltration studies.

3. Results and discussion

3.1. Time course analysis of viral replication upon transfection of SeMV wild-type icDNA

SeMV icDNA construct (SeMV IC IV pRD 400) was used for agro-infiltration of *Cyamopsis* plants as described earlier (Govind et al., 2012). Initially, the viral replication was monitored by examining CP expression as a function of time by western blot analysis of the transfected leaf samples collected from 6 to 20 days post infiltration (dpi). The expression of CP was detected at an expected size of 29 KDa in the samples isolated from 10, 15 and 20 dpi samples (Fig. 1A). There was a gradual increase in the level of CP from 10 to 20 dpi. Interestingly, CP band was not seen in 6 dpi samples indicating that the CP expression was too low to be detected at the early stages of infection (Fig. 1A). It is possible that although SeMV CP was not detected at 6 dpi, synthesis of the viral RNAs including the CP specific sgRNA was initiated at an earlier time point. Hence, in order to check for the presence of these viral RNAs, total RNA was isolated from SeMV icDNA transfected tissues at various time points (6–20 dpi) followed by reverse transcription reaction using antisense primer complementary to the 3' UTR region of the positive-sense viral genome. Since the SeMV encoded sgRNA is co-terminal with the gRNA at the 3' end, the cDNA synthesized would correspond to both (+) sgRNA as well as (+) gRNA. It must be noted here that the cDNA generated by this RT reaction was derived from viral RNAs with positive polarity since the primer used could only hybridize to the (+) sense RNA. Subsequently, PCR was carried out with this cDNA using CP gene specific primers. The full length IC IV SK + plasmid DNA template was used as a positive control for detection of 0.8 Kbp amplification product (Fig. 1B, Lane 8). Interestingly, the desired size of amplicon was detected in the samples at all the time points including that of 6 dpi indicating the presence of viral RNAs throughout the infection process (Fig. 1B, Lane 2–5). However, cDNA synthesized from the mock infiltrated leaves did not show the band corresponding to the CP PCR product (Fig. 1B, Lane 7). Further, since the agro-infiltration experiments involve the transfection of T-DNA that carries the full length icDNA, there is a possibility that the T-DNA carrying the gene of interest may be present in the transfected leaves along with the replicated viral RNA. But no detectable amplification was observed when PCR was carried out using the total RNA extracted from 6 dpi icDNA transfected samples (-RT control) as a template (Fig. 1B, Lane 6). The results confirmed that there was no/negligible contribution of the T-DNA carried over from the agro-infiltration. This suggested that although the viral-encoded CP was detected only after 6 dpi, replication of the viral RNAs in wild-type icDNA transfected plants had commenced earlier. Therefore, in order to understand the regulatory mechanisms that operate in the synthesis of various forms of viral RNA, qPCR based quantitation was used.

3.2. Standard curve generation using SeMV IC IV plasmid DNA as template

The absolute copy numbers of viral RNAs generated upon SeMV icDNA transfection were quantitated from a standard curve obtained by qPCR using the SeMV IC IV SK + plasmid DNA as template. The qPCR reaction was set up using varying concentrations of the plasmid DNA (copy numbers ranging from 300 to 3 billion) and oligonucleotide primers that were designed for the amplification of CP and MP region, of the viral gene sequence. The expected sizes of the amplicons are 167 bp and 182 bp and were termed as CP and MP amplicons respectively. Each reaction was carried out in triplicates and the average Ct values at different dilutions were recorded. As expected, the mean Ct values increased gradually with decrease in the copy numbers of the plasmid DNA samples. Further, the amplification plot for the qPCR reactions indicated an expected difference of 3 cycles (Ct values) for every 10 fold change in the copy numbers. The melting temperature (T_m) for both CP and MP amplicons were also determined. The CP and MP amplicons showed a T_m of 85 +/−1 °C and 80 +/−1 °C respectively. The mean Ct values for both these amplicons were plotted separately against the corresponding copy numbers of the plasmid DNA on a semi-logarithmic scale to generate the standard curve (Fig. 2B). Such a standard curve

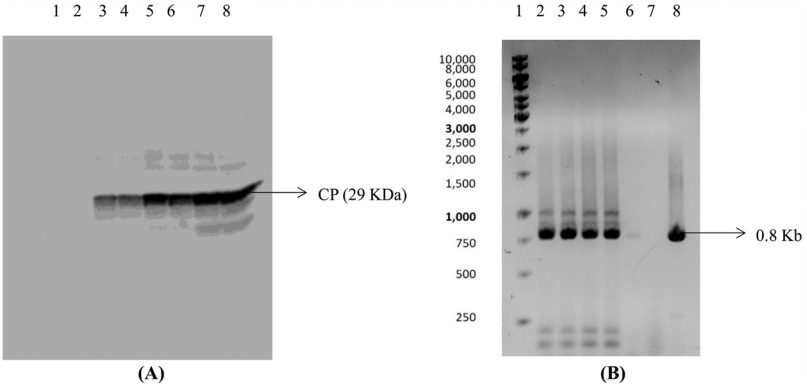

Fig. 1. Time course analysis of virus replication in wild-type icDNA transfected plants. (A) Western blot analysis was performed with the crude protein extracts of icDNA transfected leaves at 6–20 dpi using CP specific antibodies. A 29 KDa band corresponding to the expected size of the CP was detected as shown in lanes 3-8. Lanes 1–2 6 dpi samples, Lanes 3–4 10 dpi samples, Lanes 5–6 15 dpi samples, Lanes 7–8 20 dpi samples. (B) Total RNA extracted from icDNA transfected plants at 6–20 dpi were subjected to first strand cDNA synthesis using 3' UTR reverse primer (Table S1). PCR was set up with these cDNA samples using viral gene specific primers (CP sense and CP antisense, Table S1). The CP PCR product was detected at the expected 0.8 Kbp position as shown in lanes 2–5 and 8. Lane 1 1Kbp DNA ladder, Lane 2 6 dpi, Lane 3 10 dpi, Lane 4 15 dpi, Lane 5 20 dpi, Lane 6 RT (-) control, Lane 7 Mock infiltration control, Lane 8 IC IV SK + plasmid DNA positive control.

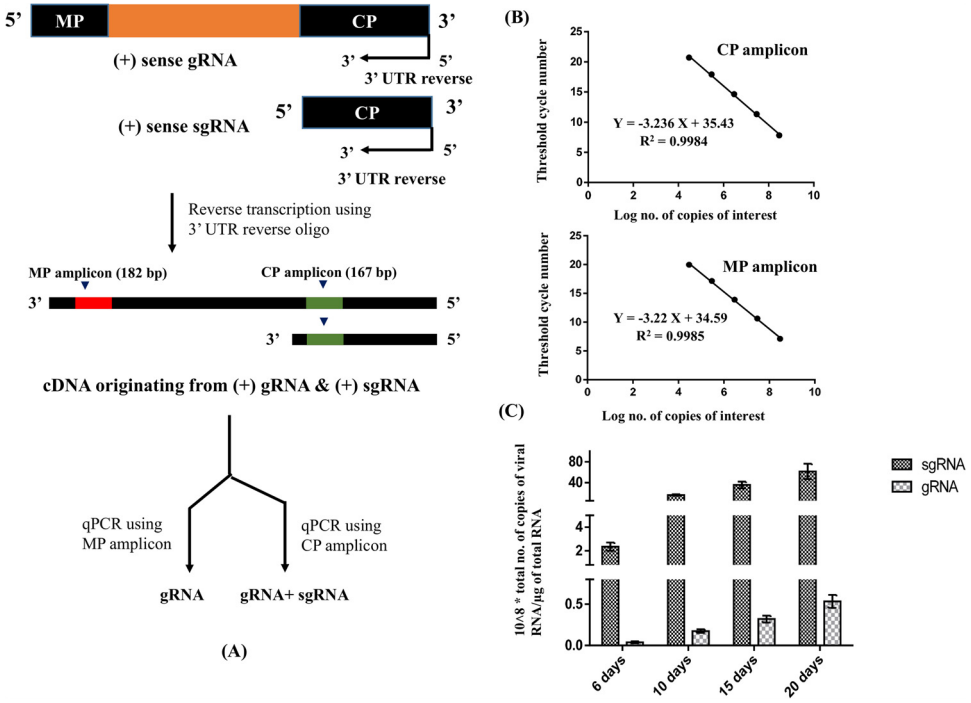

Fig. 2. (A) Strategy of quantitation of viral RNAs using qPCR. Step 1: 3' UTR reverse primer (shown in left ended arrows) was used for reverse transcription of the total RNA extracted from icDNA transfected tissues. The oligonucleotide primer used could anneal to the 3' termini of both the (+) sgRNA & (+) gRNA resulting in cDNA synthesis that corresponds to all the (+) sense viral RNAs accumulated upon transfection. Step 2: Primers corresponding to CP amplicon (167 bp) present within the CP gene sequence (enclosed within the green box in the figure) were used for qPCR with the cDNA synthesized in Step 1 as the template. Since this amplicon was part of both (+) sgRNA as well as (+) gRNA, the copy numbers derived from the mean Ct values corresponds to the aggregate of (+) sgRNA & (+) gRNA. However, MP amplicon (182 bp) designed within the MP gene sequence (enclosed within the red box in the figure) was also used for qPCR with the same cDNA as template. The mean Ct values obtained from MP amplicon was used to calculate the (+) gRNA copy numbers since this region is not present in the viral sgRNA. The (+) gRNA copy numbers were finally subtracted from those obtained using the CP amplicon which gave the copy numbers of (+) sgRNA. (B) Generation of standard curve for estimation of copy numbers of viral RNA. IC IV SK + plasmid was used as a template for generating the standard curve for qPCR experiments. A series of dilution of the template was prepared according to the desired copy numbers and qPCR was carried out using MP and CP amplicon primers (MP qPCR sense & antisense and CP qPCR sense & antisense, Table S1). The mean fractional threshold cycle numbers (Ct) obtained were recorded for both the amplicons and plotted against the corresponding copy numbers of the plasmid DNA on a semi-logarithmic scale. The slope for the standard curve and the R-squared values are shown. (C) Quantitation of the sgRNA & gRNA in wild-type icDNA transfected plants. Two independent reverse transcription reactions were carried out using the total RNA extracted from 6 to 20 dpi transfected tissues. Multiple dilutions of each set of cDNA samples were used in triplicates as template for the qPCR experiments and the mean Ct values were recorded. The sgRNA and gRNA were quantitated by plotting the mean Ct values into the standard curve of CP and MP amplicon respectively. The average copy numbers of sgRNA & gRNA at all the time intervals were plotted together in a grouped format for comparison. The levels of sgRNA and gRNA were expressed on a scale of 10^8 × copy numbers of viral RNA per µg of total RNA isolated from the icDNA transfected tissues. The error bars in the graph indicate the standard deviation in the average copy numbers of sgRNA and gRNA.

was drawn in parallel with the qPCR carried out using viral specific cDNA as template in all further experiments. The copy numbers of sgRNA and gRNA from an unknown cDNA sample that was reverse transcribed using the total RNA isolated from wild-type/mutant icDNA transfected plants were estimated by plotting the experimental Ct values onto these standard curves.

3.3. Strategy for the quantitation of viral RNA from icDNA transfected samples

Fig. 2A shows a schematic representation of the strategies employed for quantitation of gRNA & sgRNA from icDNA transfected tissues. As mentioned earlier, 3' UTR reverse primer was used to synthesize the cDNA which hybridizes at the 3' termini of both (+) sense gRNA & sgRNA. Therefore, reverse transcription using this oligo leads to the synthesis of cDNA that is proportional to the amount of gRNA and sgRNA present in the total RNA at any given time. Subsequently, qPCR was carried out using the CP and MP amplicon primers which was previously used for generation of the standard curve. As shown in Fig. 2A, the CP amplicon encompasses the sgRNA sequence which is co-terminal with the 3' terminus of the gRNA. Therefore, the copy numbers obtained by qPCR using the viral cDNA and CP amplicon primers would correspond to the cumulative copy numbers of both sgRNA & gRNA. On the other hand, the sequence of the MP amplicon as shown in the figure, is present at the 5' end of gRNA and is not a part of the sgRNA. Therefore, the qPCR using the MP amplicon primers leads to the amplification of the cDNA that corresponds to the (+) gRNA alone. The copy numbers of sgRNA were computed by subtraction of the gRNA values from the cumulative copy numbers of CP amplicon obtained from the same cDNA sample.

3.4. Quantitation of viral RNA from SeMV wild-type icDNA transfected plants

Cyamopsis plants were agro-infiltrated with SeMV icDNA and total RNA was extracted from the transfected tissues as described in the methods section. The cDNA was synthesized using 3' UTR reverse primers with 5 µg of total RNA and was diluted 1000 and 10000-fold for the qPCR reactions. The mean Ct values obtained from the qPCR experiments are tabulated (Table S2). The copy numbers of sgRNA and gRNA were calculated using the respective standard curves and recorded as viral RNA copies/µg of total RNA. These values of viral RNAs obtained upon wild-type icDNA transfection were later used for comparative analysis when the same experiments were performed with various icDNA mutants for studying the effect of specific changes in the viral genome on replication.

A comparative analysis of the sgRNA and gRNA levels in the wild-type icDNA transfected samples revealed a gradual increase in the copy numbers of sgRNA and gRNA from 6 to 20 dpi (Table 1 & Fig. 2C). However, as expected, there was a significant difference between the two forms of viral RNA throughout the infection. The levels of sgRNA at 6 dpi was approximately 60 fold higher in comparison to the gRNA which further increased to 114 fold at 20 dpi (Table 1). This is understandable as higher amounts of CP would be required at later stages of infection for encapsidation of the progeny RNAs. However, even when the level of sgRNA was higher than the gRNA by 60 fold at 6 dpi, detectable expression of CP was not observed (Fig. 1A). This could be because the sensitivity and detection limits of western blot analysis is much lower compared to the qPCR based quantitation of viral sgRNA.

Interestingly, the proteins encoded by the sgRNA in many positive-sense RNA viruses have been implicated in various functions that

Table 1
A comparative analysis of the sgRNA and gRNA levels from wild-type icDNA transfected plants. The sgRNA and gRNA levels were quantitated from the wild-type icDNA transfected tissues at 6–20 dpi and tabulated for comparison. The fold difference in the copy numbers of both forms of viral RNA is also indicated.

Wild-type icDNA transfection				
	6 dpi	10 dpi	15 dpi	20 dpi
Subgenomic RNA	(2.35 ± 0.07) $\times 10^8$	(16.10 ± 0.21) $\times 10^8$	(35.45 ± 0.39) $\times 10^8$	(61.40 ± 0.47) $\times 10^8$
Genomic RNA	(3.85 ± 0.26) $\times 10^6$	(17.45 ± 0.96) $\times 10^6$	(31.5 ± 0.84) $\times 10^6$	(53.4 ± 1.22) $\times 10^6$
Fold difference	**61.03**	**92.2**	**112.53**	**114.8**

include genome packaging, movement and pathogenesis as well as RNA recombination. The RdRps in these viruses follow a differential recognition mechanism for the sgRNA promoters that modulates the synthesis of viral proteins originating from these sgRNAs (Sztuba-Solinska et al., 2011). In addition, the *cis*-acting RNA secondary structures located upstream of the transcription initiation site play a crucial role in modulating the sgRNA levels. For instance, the brome mosaic virus (BMV) sgRNA promoter (SGP) was mapped to the sequence from nt −95 to +16 consisting of an AU-rich enhancing region, a poly (U) tract, a core region, the +1 C transcription initiation site, and a downstream sequence (Wierzchoslawski et al., 2004). The preferential binding of RdRp to the conserved enhancing region (nts −95 to −20) within the SGP was shown to greatly facilitate the synthesis of sgRNA 4 (Adkins and Kao, 1998). A similar mechanism of regulation of sgRNA synthesis might exist in SeMV which could be explored in the future.

Moreover, since the full length SeMV icDNA was used for agro-infiltration, it was necessary to calculate the copy numbers (if any) that may arise from the carryover of the infecting double-stranded DNA in the total RNA that was used for cDNA synthesis. As shown in the Table S3, the mean Ct values showed a minimal amplification when total RNA from these transfected tissues were used directly (-RT control) for qPCR. This suggested that the full length icDNA plasmid (IC IV pRD 400) that was transformed into *Agrobacterium* and used for transfection had no/negligible contribution towards the final copy numbers of viral RNAs. Further, since the cDNA was synthesized from the total RNA (host RNA included), the specificity of the primers used for the RT reaction (3' UTR reverse primer) as well as the qPCR primers towards the viral gene sequence (CP and MP amplicons) needed to be investigated. *Cyamopsis* leaves were infiltrated with *Agrobacterium* transformed with pRD 400 plasmid (vector control) and the total RNA was isolated from the leaves collected at 20 dpi followed by reverse transcription using the viral gene specific 3' UTR reverse primer. Subsequently, the cDNA synthesized (if any) was subjected to qPCR with the CP and MP amplicon primers as described for the SeMV icDNA transfected samples. The absence of any detectable amplification (Table S3) confirmed the specificity of both the qPCR primers and RT primer while annealing to the viral nucleotide sequence. These results have conclusively established that the standard curve based absolute quantitation by qPCR is an accurate and reliable method for estimation of the gRNA and sgRNA synthesized during viral infection.

3.5. Functional relevance of the RdRp-P10 interaction in viral replication in vivo

It was shown previously that SeMV encoded RdRp interacts with the viral protein P10 *via* the intrinsically disordered C-terminal domain of RdRp and the interaction led to a 8–10 fold increase in the polymerase activity *in vitro* (Govind et al., 2014). Surface plasmon resonance studies indicated that the C-terminal 72 amino acids of RdRp were crucial for the interaction with P10. Further, the interaction was shown to reduce the aggregation of RdRp that resulted in an increase in heterodimeric fraction of the RdRp-P10 complex (Bakshi et al., 2019). Such interactions between RdRp and viral-encoded ancillary proteins have been extensively studied in other positive-stranded RNA viruses like tomato bushy stunt virus (TBSV) and were shown to be crucial for VRC assembly (Rajendran and Nagy, 2004, 2006). Therefore, it was of interest to understand the relevance of the RdRp-P10 interaction in the replication of SeMV *in vivo* using the full length icDNA clone of the virus.

For this purpose, a premature stop codon was introduced within the ORF-2b gene sequence by using appropriate sense and antisense primers (Table S1) with the full length icDNA (IC IV SK+) as the template. The mutation resulted in truncation of the C-terminal domain of RdRp by 72 amino acids that would abolish the interaction with P10. Since the C-terminal sequence of RdRp overlaps with ORF-3, the mutation was planned in such a way that there was no change in the amino acid sequence of ORF-3 encoded CP. The mutant construct was confirmed by sequencing and was named RdRp STOP codon mutant for the agro-infiltration experiments in *Cyamopsis* plants.

Total RNA was isolated from the tissues agro-infiltrated with the RdRp STOP codon mutant icDNA and the gRNA and sgRNA levels were quantitated by qPCR. A comparison of the viral RNA levels in the mutant icDNA transfected plants with that of the wild-type icDNA revealed a drastic reduction in the copy numbers of both sgRNA and gRNA at all the time points tested (Fig. 3A and B). Although, a marginal increase was detected in the copy numbers of sgRNA from 6 to 20 dpi in case of the mutant icDNA infiltrated plants, there was an almost 81 and 121 fold reduction observed at 6 and 10 dpi respectively when compared to that of the wild-type icDNA transfected plants (Fig. 3A and B). It may be noted that the deletion of 72 amino acids from the C-terminus of RdRp did not affect the polymerase activity *in vitro* (Bakshi et al., 2019). Therefore, the inhibition of viral RNA synthesis observed in the mutant icDNA transfected plants could be a consequence of the loss of P10 interaction and not because of the impairment of polymerase function of RdRp *in planta*.

The replication machinery in positive-strand RNA viruses is known to exploit the host cells by subverting several host proteins and co-opting them to assemble their VRCs for the efficient synthesis of progeny RNAs (Nagy and Pogany, 2011). The host factor Tdh2/3p (yeast homologue of glyceraldehyde 3 phosphate dehydrogenase) (GAPDH) a glycolytic enzyme) was shown to be an integral part of the VRC in TBSV which binds to the 3' proximal AU pentameric sequences in negative-sense RNA leading to the selective retention of the negative strands at the replication complex (Wang and Nagy, 2008; Wang and Ahlquist, 2008). Therefore, it is likely that the truncation of the RdRp C-terminus could have not only abrogated the interaction with P10 *in vivo* but also disrupted such interactions between RdRp and co-opted host factors that may be essential for replication. A comparative analysis of the composition of VRCs in the mutant and wild-type icDNA transfected plants would provide further insights into the role of the C-terminal domain of RdRp in recruitment of these host factors. In addition, the reduced levels of gRNA in these plants could also be a consequence of the lack of encapsidation of progeny RNAs due to the substantial reduction in sgRNA levels which serves as a template for the translation of viral-encoded CP. In order to examine this, western blot analysis of the total protein extract of RdRp STOP codon mutant transfected leaves was also carried out using CP specific antibody. A faint band corresponding to the size of CP (29 KDa) was observed at 15 and 20 dpi indicating a very low level of CP expression (Fig. 4A) which further validated the effects of the mutation on viral RNA synthesis. Based on these findings, it can be suggested that the disruption of RdRp-P10 interaction results in formation of aberrant VRCs, which could lead to the conspicuous reduction in viral RNA synthesis *in vivo*.

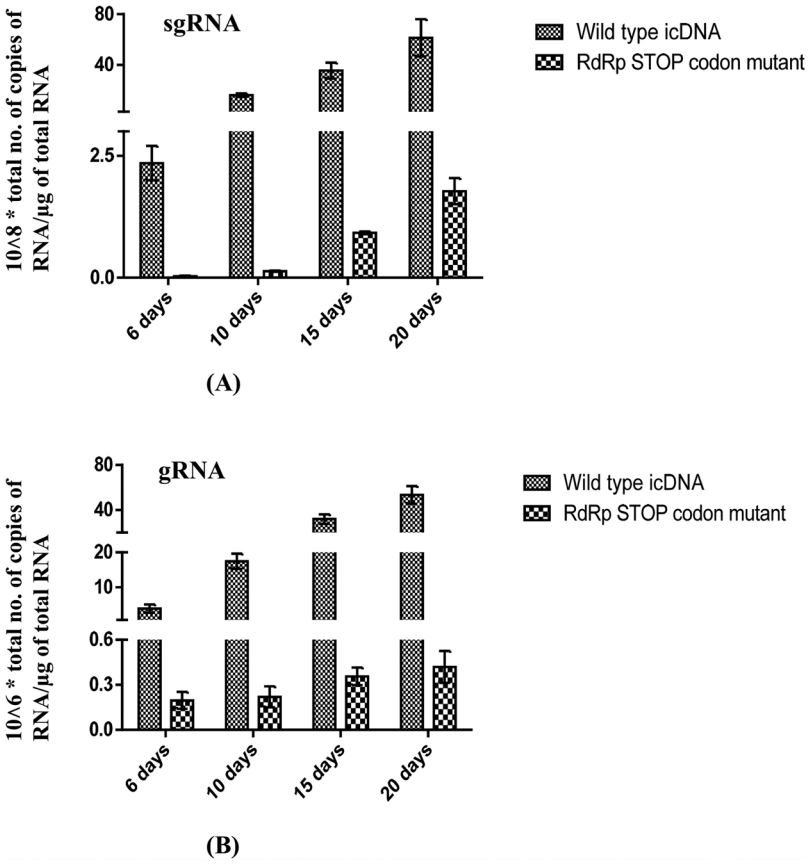

Fig. 3. Quantitation of the sgRNA & gRNA in RdRp STOP codon mutant icDNA transfected plants. (A)-(B) Two independent reverse transcription reactions were carried out using the total RNA extracted from 6 to 20 dpi transfected tissues. Multiple dilutions of each set of cDNA samples were used in triplicates as template for the qPCR experiments and the mean Ct values were recorded. The sgRNA and gRNA levels in the RdRp STOP codon mutant icDNA transfected plants at 6–20 dpi were quantitated by plotting the mean Ct values into their respective standard curves. The copy numbers of both forms of the viral RNA were compared with that obtained from the wild-type icDNA transfected plants at all the time intervals and plotted together in a grouped format for comparison. The levels of sgRNA and gRNA were expressed on a scale of 10^8 and 10^6 × copy numbers of viral RNA per µg of total RNA isolated from the icDNA transfected tissues respectively. The error bars in the graph indicate the standard deviation in the average copy numbers of sgRNA and gRNA.

3.6. Relevance of the motif E in viral replication

Based on a comparative structural and primary sequence analysis of viral RdRps, six conserved sequence motifs as A–F have been identified (Bruenn, 2003). Sequence analysis of SeMV RdRp carried out earlier had revealed the presence of motifs A-D (Govind and Savithri, 2010) including the conserved GDD motif (motif C) which is the hallmark of all viral RdRps (Choi, 2012). Interestingly, *in vitro* studies on SeMV RdRp had demonstrated the presence of a conserved motif E between 72–85 amino acids at the C-terminal disordered region of RdRp (Bakshi et al., 2019). The motif E comprises of a Y/F-aliphatic amino acid-charged amino acid and has been previously implicated in binding to the priming nucleotide during the initiation of RNA synthesis (Bressanelli et al., 2002). Further, motif E residues have been in general proposed to be a part of the initiation platform in de-novo-initiating RdRps of hepatitis C virus (HCV) and hepatitis GB virus C (GBV-C) (Bressanelli et al., 2002; Ferron et al., 2005), confirming their role in the initiation of replication. Mutation of the conserved tyrosine residue (RdRp Y480) located within the motif E of SeMV RdRp rendered the protein inactive demonstrating the importance of this motif in polymerase activity *in vitro* (Bakshi et al., 2019). Therefore, in order to decipher the relevance of this motif in viral replication *in vivo*, the conserved tyrosine residue was mutated to alanine in the full length IC IV SK+, confirmed by sequencing and named as RdRp motif E mutant for the agro-infiltration studies in *Cyamopsis* plants. Total RNA was isolated from the mutant icDNA transfected tissues and the gRNA and sgRNA levels were quantitated by qPCR. As expected, the copy numbers of both forms of the viral RNAs were found to be negligible as compared to those of wild-type icDNA transfected plants and there was no time dependent increase in their copy numbers throughout the infection (6–20 dpi) (Fig. 5A and B). This lack of increase in both the sgRNA & gRNA levels indicated the complete absence of replication, probably due to an inactive RdRp. This was further validated by the absence of CP in western blot analysis of the total protein extracted from the RdRp motif E mutant transfected tissues at 6–20 dpi (Fig. 4B). Thus, the motif E of SeMV RdRp is crucial for the polymerase activity both *in vitro* as well as *in vivo*.

3.7. Complementation studies of the RdRp mutants in vivo–rescue of viral replication

The mutational analysis on the domains/motifs of SeMV RdRp discussed so far have demonstrated the importance of the RdRp-P10 interaction and the role of motif E of RdRp in viral replication. However, it was necessary to validate these findings by complementation studies which could reverse the effect of these mutations on RNA synthesis. Therefore, it was of interest to check whether the wild-type proteins expressed from ORF-2 *in trans* could complement the effect of the deletion of C-terminal disordered domain or the mutation of Y480 of RdRp respectively, and rescue the viral replication *in vivo*.

The RdRp STOP codon mutant icDNA/RdRp motif E mutant icDNA transformants and pEAQ ORF-2 transformants were mixed together (1:1) in the induction buffer containing 150 µM acetosyringone and agro-infiltrated. This led to the co-expression from both the constructs. A comparative analysis of the viral RNA levels with that obtained when the RdRp STOP codon mutant was transfected alone is shown in Table 2A–B. It is clear that the complementation resulted in the rescue of replication and restoration of the copy numbers of both forms of viral RNA. In fact, the viral RNA levels at 10–20 dpi were almost similar or even higher than that observed for the wild-type icDNA transfected samples (Table 1). This could be due to the high levels of RdRp, protease, VPg and P10 expressed from the ORF-2 in pEAQ vector which has the 2 × 35S promoter for enhanced transcription. Similar co-infiltration experiments were also performed with *Agrobacterium* co-transformants of RdRp motif E mutant icDNA and pEAQ ORF-2. As expected, quantitation of the viral RNAs by qPCR showed a substantial increase in viral

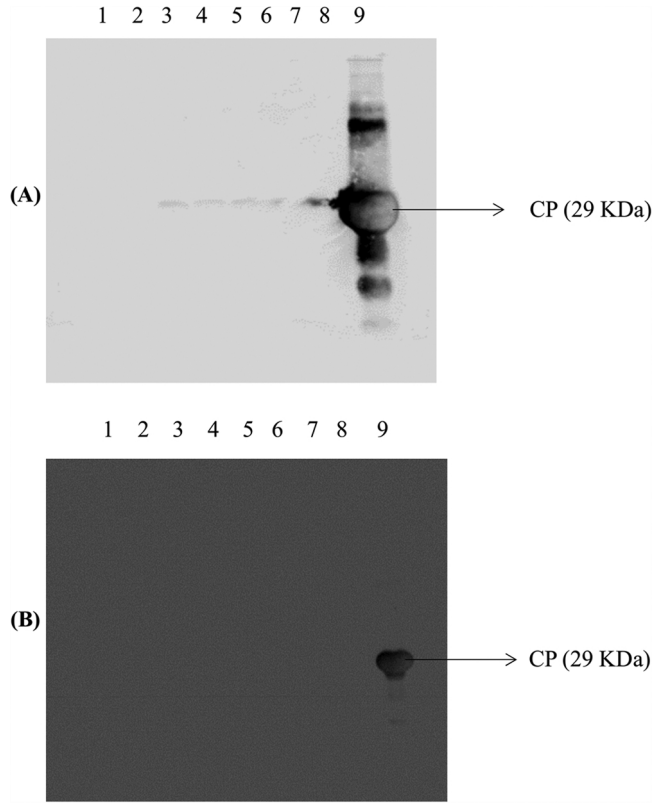

Fig. 4. Detection of CP in mutant icDNA transfected plants by western blot analysis. Western blot analysis was performed with the crude extract isolated by homogenization of RdRp STOP codon mutant (A) and RdRp motif E mutant (B) transfected tissues at 6–20 dpi using CP specific antibodies. Negligible level of CP expression was detected for RdRp STOP codon mutant (A) whereas there was no detectable CP band observed in case of RdRp motif E mutant (B). Purified native virus (29 KDa) was used a positive control. Lanes 1–2, 3–4, 5–6, 7–8 Total proteins extracted from 6, 10, 15, 20 dpi tissues respectively, Lane 9 Native virus positive control.

RNA levels (Table 3A–B). Based on these findings, it could be concluded that the wild-type RdRp expressed from pEAQ ORF-2 could functionally complement the RdRp STOP codon mutant and the inactive motif E mutant of RdRp and lead to the rescue of viral RNA synthesis *in planta*.

However, in order to rule out the possibility of a recombination between the wild-type RdRp expressed from pEAQ ORF-2 and the mutant RdRp during transfection that could also result in restoration of the viral RNA levels, cDNA synthesized from the co-infiltrated samples was amplified using gene specific primers and subjected to sequencing. The sequence analysis for both the RdRp STOP codon mutant and RdRp motif E mutant co-infiltrated samples showed that the desired mutations were retained (Fig. S2 & S3). This confirmed that the wild-type RdRp translated from ORF-2 construct was indeed responsible for the complementation of mutant RdRp which was incapable of viral RNA synthesis. Taken together, these observations provide conclusive evidence on the essential role of C-terminal disordered domain of RdRp as well as the motif E in viral replication *in vivo*.

3.8. Role of viral-encoded coat protein in replication

The fundamental role of the viral-encoded coat protein (CP) is to encapsidate the viral RNA and assemble into capsids. In addition to genome packaging, CP has also been shown to be a multifunctional protein involved in VRC assembly, viral replication and cell to cell movement. Yeast two-hybrid screening (Y2H) had previously revealed a strong interaction between SeMV CP and the viral movement protein (MP) suggesting its role in cell to cell movement of the virus (Chowdhury and Savithri, 2011). However, the viral RdRp failed to interact with CP in Y2H assay indicating the lack of direct association between CP and RdRp (Govind et al., 2014). In order to examine further if CP has any direct role in modulating viral RNA synthesis *in planta*, the start codon of ORF-3 was mutated in the SeMV IC IV SK + such that it would effectively knock-out the CP expression throughout the viral life cycle. The construct was named as CP START codon mutant and was used for agro-infiltration studies in *Cyamopsis* plants.

A comparative analysis of the sgRNA and gRNA levels with that obtained from the wild-type icDNA transfected plants is shown in Fig. 6. Interestingly, at 6 dpi the copy numbers of sgRNA and gRNA did not reveal any significant fold difference compared to the RNA levels of the wild-type icDNA transfected plants. However, once the infection progressed up to 10–20 dpi, the consequence of the absence of CP gradually gained prominence as reflected in the fold reduction in the accumulation of both forms of viral RNAs (Fig. 6). There was approximately a 100 fold reduction in the copy numbers of sgRNA and gRNA at 20 dpi due to the absence of CP which is required for the encapsidation of viral progeny RNAs. It was reported earlier that the viral-encoded sgRNA is present not only in virus infected tissues but also within virus particles of southern bean mosaic virus (SBMV) and southern cowpea mosaic virus (SCPMV). The sgRNA detected within these virus particles were in the molecular weight range of 0.3×10^6 to 0.4×10^6 and were linked to VPg at their 5' end like that of the genomic RNA (Ghosh et al., 1981; Mang et al., 1982). In addition to SBMV and SCPMV, the sgRNAs of other sobemoviruses like cocksfoot mottle virus (CfMV) were also shown to be encapsidated (Ryabov et al., 1996; Tamm et al., 1999). Therefore, the reduction of sgRNA copy numbers in CP START codon mutant icDNA transfected plants at 15 and 20 dpi could be due to the lack of encapsidation and subsequent degradation similar to that of the progeny gRNAs. Furthermore, it is evident from these results that the CP may not directly influence the activity of RdRp or the VRC assembly as the replication was unaffected during the early stages of infection (6 dpi). However, it is crucial for the packaging of viral RNAs which are otherwise susceptible to degradation by the host defence mechanisms. Thus, these findings demonstrate the role of SeMV CP in genome packaging and consequently in viral replication.

The perfect timing and optimal amount of CP synthesis is known to be essential for efficient viral infection. The CP gene expression in most positive-sense RNA viruses is tightly controlled which in turn facilitates the spatio-temporal separation of early viral genome replication from late virion assembly and movement (Ivanov and Makinen, 2012). Likewise, in many positive-sense RNA viruses, such temporal control over CP expression is achieved by the late production of CP from sgRNAs as found in the current study. Interestingly, sgRNAs are produced efficiently only when the replication cycle is already established, thus preventing premature particle assembly at the early stages of infection. However, in other positive-sense RNA viruses like potyviruses, CP expression occurs *via* proteolytic processing of a single polyprotein (Urcuqui-Inchima et al., 2001) which requires an alternate strategy to regulate the CP expression throughout the viral life cycle. The turnover of CP in such viruses is regulated either by proteosomal degradation (Hafren et al., 2010) or by post translational modifications such as phosphorylation of the protein (Ivanov et al., 2001).

The translational regulation of CP in BMV represents a valuable example of how different amounts of CP present at different time points regulate the progression of viral infection cycle (Kao et al., 2011). As the viral infection proceeds in BMV, the requirements of CP steeply increase. This is taken care by the protein itself through binding to an RNA element named SLC containing the core promoter for genomic minus-strand RNA synthesis that eventually leads to the enhancement of replication of the template for CP synthesis (Chapman and Kao, 1999). But as the levels of CP increase towards the later stages of infection, the role of CP changes from one of the replication enhancer to its inhibitor and subsequently also inhibits viral RNA translation (Yi et al., 2009a, b). A similar mechanism may be operative in the

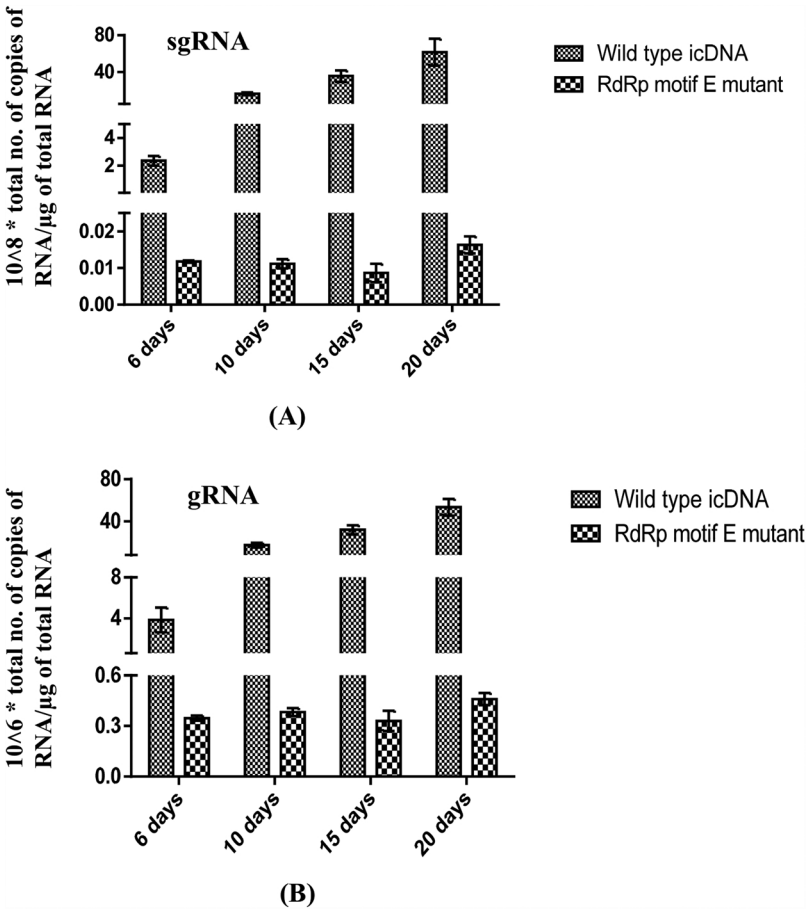

Fig. 5. Quantitation of the sgRNA & gRNA in RdRp motif E mutant icDNA transfected plants. (A)-(B) Two independent reverse transcription reactions were carried out using the total RNA extracted from 6 to 20 dpi transfected tissues. Multiple dilutions of each set of cDNA samples were used in triplicates as template for the qPCR experiments and the mean Ct values were recorded. The sgRNA and gRNA levels in the RdRp motif E mutant icDNA transfected plants at 6–20 dpi were quantitated by plotting the mean Ct values into their respective standard curves. The copy numbers of both forms of the viral RNA were compared with that obtained from the wild-type icDNA transfected plants at all the time intervals and plotted together in a grouped format for comparison. The levels of sgRNA and gRNA were expressed on a scale of 10^8 and 10^6 × copy numbers of viral RNA per µg of total RNA isolated from the icDNA transfected tissues respectively. The error bars in the graph indicate the standard deviation in the average copy numbers of sgRNA and gRNA.

Table 2
Complementation of the RdRp STOP codon mutant with pEAQ ORF-2. The viral RNA was quantitated from plants co-infiltrated with RdRp STOP codon mutant icDNA and the pEAQ ORF-2 at 6–20 dpi. The sgRNA (A) and gRNA (B) levels were compared with that obtained earlier for the RdRp STOP codon mutant transfected plants. The fold rescue indicates the increase in the copy numbers of both forms of viral RNA upon co-infiltration of ORF-2.

(A)

	Subgenomic RNA			
	6 dpi	10 dpi	15 dpi	20 dpi
RdRp STOP codon mutant	(2.9 ± 0.19) $\times 10^6$	(13.3 ± 0.98) $\times 10^6$	(90 ± 1.57) $\times 10^6$	(177 ± 3.39) $\times 10^6$
RdRp STOP codon mutant + ORF 2	(0.60 ± 0.02) $\times 10^8$	(10.35 ± 0.18) $\times 10^8$	(47.07 ± 0.26) $\times 10^8$	(62.30 ± 0.39) $\times 10^8$
Fold rescue	**20.8**	**77.8**	**52.3**	**35.19**

(B)

	Genomic RNA			
	6 dpi	10 dpi	15 dpi	20 dpi
RdRp STOP codon mutant	(1.8 ± 0.27) $\times 10^5$	(2.2 ± 0.43) $\times 10^5$	(3.5 ± 0.21) $\times 10^5$	(4.8 ± 0.37) $\times 10^5$
RdRp STOP codon mutant + ORF 2	(4.2 ± 0.14) $\times 10^6$	(11.1 ± 0.47) $\times 10^6$	(59.7 ± 0.87) $\times 10^6$	(93.1 ± 1.39) $\times 10^6$
Fold rescue	**23.3**	**50.4**	**170.5**	**194**

Table 3
Complementation of the RdRp motif E mutant with pEAQ ORF-2. The viral RNA was quantitated from plants co-infiltrated with RdRp motif E mutant icDNA and the pEAQ ORF-2 at 6–20 dpi. The sgRNA (A) and gRNA (B) levels were compared with that obtained earlier for the RdRp motif E mutant transfected plants. The fold rescue indicates the increase in the copy numbers of both forms of viral RNA upon co-infiltration of ORF-2.

(A)

	Subgenomic RNA			
	6 dpi	10 dpi	15 dpi	20 dpi
RdRp motif E mutant	(1.17 ± 0.15) $\times 10^6$	(1.10 ± 0.28) $\times 10^6$	(0.83 ± 0.11) $\times 10^6$	(1.65 ± 0.35) $\times 10^6$
RdRp motif E mutant + ORF 2	(0.03 ± 0.01) $\times 10^8$	(1.38 ± 0.15) $\times 10^8$	(15.86 ± 0.38) $\times 10^8$	(49.24 ± 0.44) $\times 10^8$
Fold rescue	**3**	**125.4**	**1910.8**	**2984.2**

(B)

	Genomic RNA			
	6 dpi	10 dpi	15 dpi	20 dpi
RdRp motif E mutant	(3.41 ± 0.58) $\times 10^5$	(3.82 ± 0.72) $\times 10^5$	(3.38 ± 0.74) $\times 10^5$	(4.67 ± 0.29) $\times 10^5$
RdRp motif E mutant + ORF 2	(1.31 ± 0.15) $\times 10^6$	(1.92 ± 0.12) $\times 10^6$	(71.34 ± 0.89) $\times 10^6$	(345.2 ± 0.77) $\times 10^6$
Fold rescue	**3.8**	**4.97**	**210.9**	**739.1**

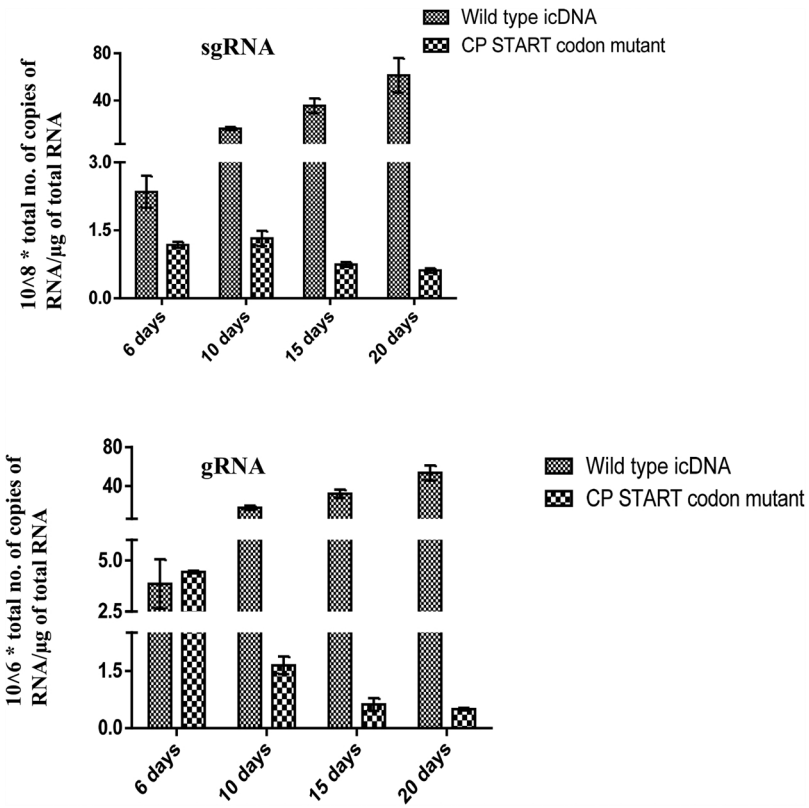

Fig. 6. Quantitation of the sgRNA & gRNA in CP START codon mutant icDNA transfected plants. (A)-(B) Two independent reverse transcription reactions were carried out using the total RNA extracted from 6 to 20 dpi transfected tissues. Multiple dilutions of each set of cDNA samples were used in triplicates as template for the qPCR experiments and the mean Ct values were recorded. The sgRNA and gRNA levels in the CP START codon mutant icDNA transfected plants at 6–20 dpi were quantitated by plotting the mean Ct values into their respective standard curves. The copy numbers of both forms of the viral RNA were compared with that obtained from the wild-type icDNA transfected plants at all the time intervals and plotted together in a grouped format for comparison. The levels of sgRNA and gRNA were expressed on a scale of 10^8 and 10^6 × copy numbers of viral RNA per µg of total RNA isolated from the icDNA transfected tissues respectively. The error bars in the graph indicate the standard deviation in the average copy numbers of sgRNA and gRNA.

translational regulation of SeMV CP.

4. Conclusions

In summary, the work presented in this paper established qPCR as a reliable tool for quantitation of viral RNAs synthesized upon agro-infiltration of full length SeMV icDNA in *Cyamopsis* plants. The results obtained clearly demonstrate the requirement of the interaction between RdRp and P10 *via* the intrinsically disordered C-terminal domain of RdRp in viral replication and progression of infection *in vivo*. In addition, the motif E located at the C-terminus of RdRp was shown to be indispensable for viral RNA synthesis. Although the viral-encoded CP was found to be dispensable for replication, an increased level of CP expression was shown to be crucial for genome encapsidation towards the later stages of viral infection. Overall, this quantitation method could be used as a universal tool for studying similar structure-function relationship of viral-encoded genes and their role in replication for other plant infecting positive-strand RNA viruses as well.

Funding information

We thank Department of Biotechnology (DBT), India, (Grant ID No.BT/PR6711/NNT/28/622/2012), Department of Science and Technology (DST), India, (Grant ID- No.SR/S2/JCB-60/2007) and Indian Institute of Science, India for financial support. HSS acknowledges DST for J C Bose fellowship and Indian National Science Academy for support. AB acknowledges Council of Scientific and Industrial Research (CSIR), India for Senior Research Fellowship.

Conflict of interest

The authors declare that they have no conflicts of interest with the contents of this article.

Acknowledgements

We thank Dr. Kristiina Mäkinen for providing the pEAQ construct. We thank Dr. Kunduri Govind for the full length SeMV icDNA construct and his guidance in planning the *in vivo* experiments. We also thank Dr. G.P. Vishnu Vardhan and Ms. Sushmitha C for their help and assistance during transfection experiments.

Appendix A. Supplementary data

Supplementary material related to this article can be found, in the online version, at doi:https://doi.org/10.1016/j.virusres.2019.05.003.

References

Adkins, S., Kao, C.C., 1998. Subgenomic RNA promoters dictate the mode of recognition by bromoviral RNA-dependent RNA polymerases. Virology 252, 1–8.
Bakshi, A., Sridhar, S., Sistla, S., Savithri, H.S., 2019. Interaction of the intrinsically disordered C-terminal domain of the sesbania mosaic virus RNA-dependent RNA polymerase with the viral protein P10 in vitro: modulation of the oligomeric state and polymerase activity. Arch. Virol. 164, 971–982.
Bressanelli, S., Tomei, L., Rey, F.A., De Francesco, R., 2002. Structural analysis of the hepatitis C virus RNA polymerase in complex with ribonucleotides. J. Virol. 76, 3482–3492.
Bruenn, J.A., 2003. A structural and primary sequence comparison of the viral RNA-dependent RNA polymerases. Nucleic Acids Res. 31, 1821–1829.
Chapman, M.R., Kao, C.C., 1999. A minimal RNA promoter for minus-strand RNA synthesis by the brome mosaic virus polymerase complex. J. Mol. Biol. 286, 709–720.
Choi, K.H., 2012. Viral polymerases. Adv. Exp. Med. Biol. 726, 267–304.
Chowdhury, S.R., Savithri, H.S., 2011. Interaction of Sesbania mosaic virus movement protein with the coat protein–implications for viral spread. FEBS J. 278, 257–272.
de Castro, I.F., Volonte, L., Risco, C., 2013. Virus factories: biogenesis and structural design. Cell. Microbiol. 15, 24–34.
den Boon, J.A., Diaz, A., Ahlquist, P., 2010. Cytoplasmic viral replication complexes. Cell Host Microbe 8, 77–85 ref.
Eskelin, K., Suntio, T., Hyvarinen, S., Hafren, A., Makinen, K., 2010. Renilla luciferase-based quantitation of Potato virus A infection initiated with Agrobacterium infiltration of N. benthamiana leaves. J. Virol. Methods 164, 101–110.
Ferron, F., Bussetta, C., Dutartre, H., Canard, B., 2005. The modeled structure of the RNA dependent RNA polymerase of GBV-C virus suggests a role for motif E in Flaviviridae RNA polymerases. BMC Bioinformatics 6, 255.

Ghosh, A., Rutgers, T., Ke-Qiang, M., Kaesberg, P., 1981. Characterization of the coat protein mRNA of southern bean mosaic virus and its relationship to the genomic RNA. J. Virol. 39, 87–92.
Govind, K., Savithri, H.S., 2010. Primer-independent initiation of RNA synthesis by SeMV recombinant RNA-dependent RNA polymerase. Virology 401, 280–292.
Govind, K., Makinen, K., Savithri, H.S., 2012. Sesbania mosaic virus (SeMV) infectious clone: possible mechanism of 3' and 5' end repair and role of polyprotein processing in viral replication. PLoS One 7, e31190.
Govind, K., Bakshi, A., Savithri, H.S., 2014. Interaction of Sesbania mosaic virus (SeMV) RNA-dependent RNA polymerase (RdRp) with the p10 domain of polyprotein 2a and its implications in SeMV replication. FEBS Open Bio 4, 362–369.
Hafren, A., Hofius, D., Ronnholm, G., Sonnewald, U., Makinen, K., 2010. HSP70 and its cochaperone CPIP promote potyvirus infection in Nicotiana benthamiana by regulating viral coat protein functions. Plant Cell 22, 523–535.
Ivanov, K.I., Makinen, K., 2012. Coat proteins, host factors and plant viral replication. Curr. Opin. Virol. 2, 712–718.
Ivanov, K.I., Puustinen, P., Merits, A., Saarma, M., Makinen, K., 2001. Phosphorylation down-regulates the RNA binding function of the coat protein of potato virus A. J. Biol. Chem. 276, 13530–13540.
Kao, C.C., Ni, P., Hema, M., Huang, X., Dragnea, B., 2011. The coat protein leads the way: an update on basic and applied studies with the Brome mosaic virus coat protein. Mol. Plant Pathol. 12, 403–412.
Lokesh, G.L., Gopinath, K., Satheshkumar, P.S., Savithri, H.S., 2001. Complete nucleotide sequence of Sesbania mosaic virus: a new virus species of the genus Sobemovirus. Arch. Virol. 146, 209–223.
Mang, K.Q., Ghosh, A., Kaesberg, P., 1982. A comparative study of the cowpea and bean strains of southern bean mosaic virus. Virology 116, 264–274.
Nagy, P.D., Pogany, J., 2011. The dependence of viral RNA replication on co-opted host factors. Nature reviews. Microbiology 10, 137–149.
Nair, S., Savithri, H.S., 2010. Processing of SeMV polyproteins revisited. Virology 396, 106–117.
Rajendran, K.S., Nagy, P.D., 2004. Interaction between the replicase proteins of Tomato bushy stunt virus in vitro and in vivo. Virology 326, 250–261.
Rajendran, K.S., Nagy, P.D., 2006. Kinetics and functional studies on interaction between the replicase proteins of Tomato Bushy Stunt Virus: requirement of p33:p92 interaction for replicase assembly. Virology 345, 270–279.
Reusken, C.B., Neeleman, L., Bol, J.F., 1994. The 3'-untranslated region of alfalfa mosaic virus RNA 3 contains at least two independent binding sites for viral coat protein. Nucleic Acids Res. 22, 1346–1353.
Ryabov, E., Krutov, A., Novikov, V., Zheleznikova, O., Morozov, S.Y., Zavriev, S., 1996. Nucleotide sequence of RNA from the sobemovirus found in infected cocksfoot shows a luteovirus-like arrangement of the putative replicase and protease genes. Phytopathology 86, 391–397.
Satheshkumar, P.S., Lokesh, G.L., Savithri, H.S., 2004. Polyprotein processing: cis and trans proteolytic activities of Sesbania mosaic virus serine protease. Virology 318, 429–438.
Shulla, A., Randall, G., 2016. (+) RNA virus replication compartments: a safe home for (most) viral replication. Curr. Opin. Microbiol. 32, 82–88.
Sztuba-Solinska, J., Stollar, V., Bujarski, J.J., 2011. Subgenomic messenger RNAs: mastering regulation of (+)-strand RNA virus life cycle. Virology 412, 245–255.
Tamm, T., Makinen, K., Truve, E., 1999. Identification of genes encoding for the cocksfoot mottle virus proteins. Arch. Virol. 144, 1557–1567.
Urcuqui-Inchima, S., Haenni, A.L., Bernardi, F., 2001. Potyvirus proteins: a wealth of functions. Virus Res. 74, 157–175.
Van Larebeke, N., Engler, G., Holsters, M., Van den Elsacker, S., Zaenen, I., Schilperoort, R.A., Schell, J., 1974. Large plasmid in Agrobacterium tumefaciens essential for crown gall-inducing ability. Nature 252, 169–170.
Wang, X., Ahlquist, P., 2008. Filling a GAP(DH) in asymmetric viral RNA synthesis. Cell Host Microbe 3, 124–125.
Wang, R.Y., Nagy, P.D., 2008. Tomato bushy stunt virus co-opts the RNA-binding function of a host metabolic enzyme for viral genomic RNA synthesis. Cell Host Microbe 3, 178–187.
Weiner, M.P., Costa, G.L., Schoettlin, W., Cline, J., Mathur, E., Bauer, J.C., 1994. Site-directed mutagenesis of double-stranded DNA by the polymerase chain reaction. Gene 151, 119–123.
Wierzchoslawski, R., Dzianott, A., Bujarski, J., 2004. Dissecting the requirement for subgenomic promoter sequences by RNA recombination of brome mosaic virus in vivo: evidence for functional separation of transcription and recombination. J. Virol. 78, 8552–8564.
Yi, G., Letteney, E., Kim, C.H., Kao, C.C., 2009a. Brome mosaic virus capsid protein regulates accumulation of viral replication proteins by binding to the replicase assembly RNA element. RNA 15, 615–626.
Yi, G., Vaughan, R.C., Yarbrough, I., Dharmaiah, S., Kao, C.C., 2009b. RNA binding by the brome mosaic virus capsid protein and the regulation of viral RNA accumulation. J. Mol. Biol. 391, 314–326.